Research Article

Development and Physicochemical Characterization of An Empagliflozin-Loaded Oral Nanoemulsion: Formulation Optimization, in Vitro Release Kinetics, and Exploratory Ex Vivo Intestinal Permeation

Satya Prakash[1], Garima Gupta[2], Mohammad Rashid[3*], Swamita Arora[4] , Sanjar Alam[4]

[1]Research Scholar, Department of Pharmacy, Monad University, Hapur, U.P.- 201310
[2]Professor, Department of Pharmacy, Monad University, Hapur, U.P.- 201310
[3*] Associate Professor, R V Northland Institute, Greater Noida - 201 306, India. ORCID- 0009-0005-5774-1728
[4] Professor, R.V. Northland Institute, G.B. Nagar, Dadri, Greater Noida. U.P.-203207

*Corresponding Author
Dr. Mohammad Rashid, Email: dr.r.khan01@gmail.com

Abstract

Background: Empagliflozin is a selective sodium–glucose cotransporter-2 (SGLT2) inhibitor used in the management of type 2 diabetes mellitus. Its intestinal permeability presents an opportunity for improving oral drug delivery through lipid-based nanocarriers. The present study aimed to develop, screen, and characterize an empagliflozin-loaded oral nanoemulsion and evaluate its in vitro drug release and exploratory ex vivo intestinal permeation performance.

Methods: Empagliflozin-loaded nanoemulsions were prepared using Capryol 90 as the oil phase, Tween 80 as the surfactant, and Transcutol P as the cosurfactant. Excipient screening and pseudo-ternary phase diagrams guided formulation development. Eight trial formulations (NE1–NE8) were subjected to preliminary physical examination and stress-stability screening. Selected formulations were evaluated for physicochemical characteristics, including droplet size, polydispersity index, zeta potential, viscosity, optical transmittance, and drug content. In vitro drug release was assessed using a diffusion-based method, while ex vivo intestinal permeation was compared with unformulated empagliflozin. Drug-content retention was also monitored over six months.

Results: The selected nanoemulsion exhibited a Z-average hydrodynamic diameter of 227.5 nm and a polydispersity index of 0.270. The Tween 80:Transcutol P ratio of 3:1 produced the largest estimated nanoemulsion-forming region (16.48%). At 12 h, cumulative apparent drug release reached 98.1% from the nanoemulsion compared with 63.2% from the unformulated suspension. The Higuchi transformation provided the strongest descriptive fit across the complete release profile (R^2 = 0.9900). Exploratory ex vivo intestinal permeation reached 7563.33 µg/cm² for the nanoemulsion and 5353.33 µg/cm² for unformulated empagliflozin at 24 h, corresponding to a 1.41-fold difference in cumulative transport. Drug content decreased from 99.07% to 97.64% during six months of storage, representing 98.56% retention relative to the initial value.

Conclusion: The empagliflozin-loaded nanoemulsion demonstrated favorable physicochemical characteristics, increased apparent drug release, and greater cumulative intestinal drug transfer than the unformulated suspension under the investigated experimental conditions. These findings support further evaluation of lipid-based nanoemulsions for oral empagliflozin delivery. Additional studies confirming intestinal tissue integrity, reproducibility, long-term formulation stability, and in vivo pharmacokinetic performance are required to establish improved oral bioavailability and therapeutic efficacy.

Keywords: Empagliflozin, Oral nanoemulsion, Type 2 diabetes mellitus, Capryol 90, Tween 80, Transcutol P, Drug release kinetics, Ex vivo intestinal permeation, Formulation stability.

1. Introduction

Type 2 diabetes mellitus remains a major therapeutic challenge because sustained glycaemic control often requires long-term oral treatment. Empagliflozin is a selective sodium glucose cotransporter-2 inhibitor used in type 2 diabetes. It lowers plasma glucose through an insulin-independent mechanism by reducing renal glucose reabsorption and increasing urinary glucose excretion. Its clinical value also extends to cardiovascular and renal protection in appropriate patient populations [1].

The biopharmaceutical profile of empagliflozin requires careful interpretation. Earlier formulation literature often described the drug as poorly soluble. More recent evidence provides a clearer classification. A 2025 biowaiver monograph concluded that empagliflozin satisfies the dose-based high-solubility criterion but does not meet the high-permeability criterion. It is therefore classified as a Biopharmaceutics Classification System Class III drug. Low intestinal permeability, together with transporter-mediated efflux, represents a more relevant oral-delivery barrier than aqueous solubility alone [2].

This distinction changes the formulation objective. An oral delivery system for empagliflozin should maintain the drug in a readily transferable state after gastrointestinal dilution and support efficient contact with the intestinal membrane. It should remain physically stable, resist precipitation, and provide reproducible dispersion. Increasing apparent solubility alone does not address these requirements.

Lipid-based systems provide a practical approach to oral drug delivery. Oils, surfactants, and cosurfactants form dispersed structures with a large interfacial area after contact with aqueous media. Their performance depends on drug partitioning, excipient composition, interfacial behaviour, dilution stability, and gastrointestinal processing [3–4]. Nanoemulsions provide small dispersed droplets and a high surface-to-volume ratio. These properties support rapid dispersion and drug transfer when the formulation remains stable after physiological dilution [5–6].

Recent studies support nano-enabled delivery of empagliflozin. Sinha et al. incorporated empagliflozin-loaded chitosan-alginate nanoparticles into an orodispersible film. The system produced a 7.2-fold increase in permeability and a modest improvement in systemic exposure compared with the free-drug film [7]. Wagh et al. developed TPGS polymeric micelles with a mean size close to 9 nm and reported a 3.12-fold increase in AUC compared with an empagliflozin suspension [8]. Hammad et al. also reported improved delivery of empagliflozin using a cubosomal dual-drug platform [9].

Nanoemulsion-based work has also emerged. Alhakamy et al. developed an empagliflozin nanoemulsion with a mean particle size of 136.1 nm, a PDI of 0.281, and a zeta potential of −23.9 mV. The work confirmed the formulation feasibility of empagliflozin nanoemulsions, although its therapeutic objective differed from oral antidiabetic delivery [10].

More direct evidence appeared in 2026. Hathout et al. developed an empagliflozin self-microemulsifying system containing Tween 60, Transcutol, Capryol, and ethyl oleate. After aqueous dispersion, the formulation produced droplets of 31.2 nm with a PDI of 0.292. It increased ileal and colonic absorption by approximately 1.9-fold and 1.85-fold, respectively. The formulation also increased the area under the blood-glucose-reduction curve by approximately 1.45-fold compared with aqueous empagliflozin dispersion [11].

These findings establish the potential of lipid-based empagliflozin delivery. They also define a clear research need. Formulation performance depends strongly on the selected oil, surfactant, cosurfactant, and their relative proportions. A composition reported for one self-emulsifying system does not define the optimum composition for another. Phase behaviour, drug loading, droplet size, polydispersity, dilution resistance, release, and intestinal transport all change with formulation composition.

A systematic mixture-design approach therefore offers a stronger development strategy than empirical formulation selection. D-optimal mixture design is particularly suitable for lipid-based systems because formulation components are interdependent proportions constrained by a fixed total [12].

A further gap lies in integrated performance assessment. Many formulation studies examine particle size, release, or pharmacokinetics as isolated endpoints. For a BCS Class III drug, improved release does not itself prove improved intestinal transport. A stronger experimental approach links excipient screening and phase mapping with statistical optimization, physicochemical characterization, post-dilution behaviour, comparative release, and direct intestinal-permeation assessment.

The present study therefore developed an oral empagliflozin nanoemulsion based on Capryol 90, Tween 80, and Transcutol P. The formulation domain was defined through excipient screening and pseudo-ternary phase mapping, followed by statistical mixture optimization. The optimized system was characterized for droplet size, PDI, surface charge, physicochemical stability, drug content, and dilution behaviour. Its in-vitro release profile was compared with unformulated empagliflozin. Ex-vivo intestinal transport was then assessed through cumulative permeation, steady-state flux, apparent permeability coefficient, and permeation-enhancement ratio. The study was designed to determine whether rational nanoemulsion engineering improves the intestinal-delivery performance of empagliflozin rather than simply producing a smaller dispersed droplet.

2. Materials and Methods

2.1. Study design

The study used a sequential approach to develop and select an empagliflozin-loaded oil-in-water nanoemulsion for oral delivery. Drug identity, compatibility, analytical performance and solubility were assessed first. Oil, surfactant and cosurfactant candidates were screened, followed by pseudo-ternary phase mapping. Eight trial nanoemulsions were prepared from the selected composition region. Centrifugation and temperature-cycling studies guided the initial selection of three stable formulations. Their physicochemical properties, in vitro drug release and ex vivo intestinal transport were compared to select a lead formulation. Confirmatory evaluation and stability testing were then assigned to the lead formulation. No statistical mixture design or response-surface optimization was performed. The selection procedure followed published excipient-screening and phase-mapping strategies [1,2].

2.2. Materials and procurement

Empagliflozin was obtained from [supplier, city, country, grade, batch number and certificate of analysis]. Candidate oils included Capryol 90, Sefsol 218, Labrafac-type lipid, ethyl oleate, oleic acid and medium-chain triglycerides. Candidate surfactants included Tween 80, Tween 20, Labrasol, Kolliphor RH40 and Kolliphor HS15. Candidate cosurfactants included Transcutol P, polyethylene glycol 400, polyethylene glycol 200 and propylene glycol. The source draft reports Central Drug House, New Delhi, India, as the supplier for the screening excipients. Confirm the commercial grade, source and batch of each material. Methanol and other reagents were analytical grade. Purified or double-distilled water was used [select one consistently from laboratory records].

2.3. Preformulation and analytical characterization

2.3.1. Physical examination and preliminary drug identity

The received drug was examined for appearance, colour and melting behaviour. UV absorption, Fourier-transform infrared (FTIR) spectroscopy and differential scanning calorimetry (DSC) were used to support preliminary identity and thermal assessment. Record the instrument models and calibration status: [instrument details].

2.3.2. Development and validation of the UV-visible assay

A primary stock of empagliflozin was prepared in methanol. Working standards covered 2–12 µg/mL at a minimum of six concentration levels. A representative solution was scanned from 200 to 400 nm against the relevant blank. The draft reports an absorption maximum of 213 nm. This wavelength must be confirmed using the original spectra and matrix-interference study because a later section states 213 nm. Use one validated wavelength consistently for drug assay and release/permeation sample analysis, or provide separately validated methods for different matrices. Calibration was assessed by least-squares regression. Validation included range, accuracy, repeatability, intermediate precision, specificity and robustness, with detection and quantitation limits where relevant. Drug-free placebo and each relevant receptor or extraction medium were tested for spectral interference. At a low UV wavelength, a stability-indicating chromatographic method should be considered when degradation products or excipient background cannot be resolved. Analytical validation followed relevant ICH Q2(R2) principles [3].

2.3.3. Aqueous solubility and partition behaviour

Equilibrium solubility was assessed in water and acidic and near-intestinal pH media [buffer identity, pH, volume, temperature, agitation, duration and validation of equilibrium]. Excess drug was equilibrated with each medium, separated from undissolved material by centrifugation or validated filtration, and quantified after suitable dilution. The apparent n-octanol–aqueous distribution was estimated by a shake-flask procedure using mutually saturated phases. Concentrations after equilibration were determined analytically. The ratio was calculated as P = C(octanol)/C(aqueous), with log P = log10(P). For buffered aqueous medium, report log D at the measured pH rather than treating the result as an intrinsic neutral-species log P. Confirm mass balance and test temperature.

2.3.4. Drug–excipient compatibility

The FTIR spectra of empagliflozin and representative drug–excipient blends were recorded over approximately 4000–400 cm^{-1}. DSC thermograms were obtained for pure drug and selected blends using [pan type, sample mass, temperature range, heating rate and purge atmosphere]. Compatibility screening included Capryol 90, Sefsol 218, Tween 80, Transcutol P and selected surfactant–cosurfactant blends. Spectral shifts or thermal transitions were interpreted alongside other evidence and not treated alone as proof of chemical reaction.

2.4. Screening and selection of Nanoemulsion components

2.4.1. Solubility screening of oils, surfactants and cosurfactants

Excess empagliflozin was added separately to candidate oils, surfactants and cosurfactants. The mixtures were agitated under controlled conditions [temperature, time and speed] and centrifuged. Clear supernatants were diluted in the validated solvent and assayed. Measurements were performed in triplicate, as stated in the draft. Selection considered measured solubility, emulsification, optical clarity, dilution robustness and suitability for oral administration, not solubility alone [1].

2.4.2. Selection of the working excipient system

Capryol 90, Tween 80 and Transcutol P were carried forward for phase mapping. The final rationale and experimental values supporting this selection should be reported in the Results section. Record the excipient grades and intended oral exposure per dose.

2.5. Pseudo-ternary phase behaviour

Tween 80 and Transcutol P were blended at mass ratios of 1:1, 2:1, 3:1, 1:2 and 1:3 (Smix). Capryol 90 and each Smix were combined over oil-to-Smix mass ratios from 9:1 to 1:9. Water was titrated into each mixture under gentle agitation at room temperature [actual temperature and equilibration interval]. Each system was inspected for clarity, translucency, flow, turbidity and phase separation. Homogeneous transparent or translucent regions were provisionally marked on pseudo-ternary plots, and regions near visible phase boundaries were excluded

from candidate selection. Visual clarity alone does not prove nanometre-scale droplets. Droplet-size analysis must confirm the classification of shortlisted compositions [1,2].

2.6. Preparation of eight empagliflozin-loaded trial nanoemulsions

Eight candidate formulations, NE1–NE8, were selected from the experimental phase region. The proposed drug loading was 10 mg/mL. Empagliflozin was mixed with Capryol 90, Tween 80 and Transcutol P until a homogeneous phase formed. Water was added gradually under magnetic stirring. The addition order, temperature, stirrer speed, mixing time and batch volume were held constant. Matched drug-free placebos were prepared for matrix controls. Trial formulations were inspected for precipitation, creaming, cracking, turbidity and phase separation after drug loading and dilution.

Table 1. Proposed compositions of eight empagliflozin-loaded Nanoemulsion trial formulations (NE1–NE8).

Formulation	Capryol 90 (% w/w)	Tween 80 (% w/w)	Transcutol P (% w/w)	Water (% w/w)	Empagliflozin
NE1	5	30.00	10.00	55	10 mg/mL target
NE2	10	30.00	10.00	50	10 mg/mL target
NE3	15	30.00	10.00	45	10 mg/mL target
NE4	20	30.00	10.00	40	10 mg/mL target
NE5	10	37.50	12.50	40	10 mg/mL target
NE6	15	37.50	12.50	35	10 mg/mL target
NE7	20	37.50	12.50	30	10 mg/mL target
NE8	25	37.50	12.50	25	10 mg/mL target

2.7. Stress-stability screening and preliminary selection

2.7.1. Centrifugation test

Each trial formulation was centrifuged at [relative centrifugal force (×g), duration and temperature]. The samples were inspected for creaming, cracking, phase separation and drug precipitation. Report relative centrifugal force rather than rpm alone, or state rotor radius.

2.7.2. Heating–cooling cycles

The formulations underwent six alternating cycles between 4 ± 2 °C and 40 ± 2 °C. Each temperature stage lasted 48 h, as specified in the draft. The definition of one complete cycle, total exposure time and observation schedule must be confirmed. Visual changes and drug precipitation were recorded after each cycle.

2.7.3. Freeze–thaw cycles

The formulations underwent three cycles between −20 ± 2 °C and 25 ± 2 °C, with a 24 h hold at each stage. Samples were evaluated after thawing for irreversible separation, aggregation and visible precipitation. These are accelerated physical stress challenges, not proof of thermodynamic stability or an expiry period [2].

2.7.4. Selection of three stable trial formulations

A formulation failed the initial screen if it showed irreversible phase separation, cracking or visible drug precipitation under the predefined conditions. Of the eligible formulations, three were advanced for comparative characterization using prespecified secondary criteria [record the rule and actual codes]. The pass/fail data for all eight formulations must be reported to make the selection reproducible.

2.8. Comparative physicochemical characterization of three selected formulations

Immediately after preparation, the three selected nanoemulsions were examined for appearance, pH, apparent viscosity, refractive index, optical transmittance, drug content, droplet size, polydispersity index (PDI) and zeta potential. Hydrodynamic diameter and PDI were measured by dynamic light scattering at approximately 25 °C after a validated dilution, where needed. Zeta potential was measured under controlled medium and dilution conditions and interpreted together with steric stabilization from Tween 80. pH was measured using a calibrated meter. Viscosity was recorded at 25 ± 0.5 °C, with 50 rpm as the source-draft comparison setting. Refractive index was measured at 25 ± 0.5 °C. Percentage transmittance was recorded at 650 nm against water. Replicate counts, instrument details and dilution factors must be supplied. Drug content was calculated as 100 × (measured drug amount)/(nominal drug amount), using the validated matrix-specific assay. Entrapment efficiency was not claimed without a validated separation of free and associated drug.

2.9. Comparative in vitro drug release

The three shortlisted formulations were evaluated using a diffusion-based in vitro release setup. Equal nominal drug doses were placed in donor compartments. Receptor medium, membrane type, membrane compatibility, receptor volume, effective area, temperature, agitation and sampling intervals were standardized [enter values]. Samples were quantified by a matrix-validated procedure, and cumulative release was corrected for serial

withdrawal and replacement. Profiles were presented as percent dose released against time. Candidate release models were assessed using their assumptions and goodness of fit, without claiming a specific transport mechanism from a fit alone.

2.10. Comparative ex vivo intestinal permeation

An everted rat intestinal sac model was planned to compare intestinal transport of the three selected nanoemulsions. Tissue preparation requires documented ethics approval, experimental-animal provenance, intestinal segment selection and viability or barrier-integrity checks. After collection, the intestine was transferred to cold oxygenated buffer, flushed and everted gently. Each sac contained a fixed serosal-buffer volume and was exposed on the mucosal side to a defined equivalent empagliflozin dose [insert exposure area, volume, temperature, oxygenation, sampling times and animal-level replication]. Unformulated empagliflozin was tested at a matched dose or donor concentration as the comparator. Flux, Jss = (dQ/dt)/A, was estimated only where the permeation curve contained a defensible linear region. Apparent permeability was calculated as Papp = Jss/C0 when donor concentration and units supported the calculation. Enhancement ratio was defined as Papp(nanoemulsion)/Papp(unformulated). Specify how tissues were treated as biological replicates and how tissue damage was excluded.

The uploaded draft also included Franz-cell skin permeation. As the stated target is enhanced oral delivery, skin permeation is not used to rank the oral nanoemulsions. Its original plan is preserved in the editorial record at the end of this document for possible use in a separate transdermal study.

2.11. Comparative ranking and selection of one lead formulation

Only formulations passing the physical stress criteria were eligible for final selection. The three shortlisted systems were compared by a predefined decision rule combining droplet size and PDI, drug-content recovery, dilution robustness, in vitro release and intestinal permeation. Experimental safety and feasibility limits took precedence over numerical scores. If several formulations satisfied all limits, use a fixed, prospectively documented weighted score. Do not adjust weights after reviewing outcomes. Weighting values, acceptance thresholds and any sensitivity analysis must be disclosed. The highest eligible score defined the lead formulation. Report it as the selected or best-performing formulation within the eight tested compositions, not as a statistically globally optimized composition.

2.12. Lead formulation confirmation

The selected formulation was prepared in [number] independent batches using the same method and composition. Batch-to-batch drug content, droplet size, PDI, appearance and other critical measurements were compared with prespecified specifications. Confirmatory FTIR, DSC or droplet morphology studies should be described here only if actually performed. Record whether the final formula was changed after screening. Any modified formula must undergo the relevant screening and comparison again.

2.13. Stability evaluation and shelf-life assessment

2.13.1. Packaging and storage

The lead formulation was filled into tightly closed, light-protective containers [container material, headspace, fill volume and closure]. The source draft proposed accelerated storage at 40 ± 2 °C/75 ± 5% relative humidity for six months, assessed at 0, 1, 3 and 6 months. Add long-term stability at a justified intended market/storage condition, with the associated schedule and testing frequency. State the number of independently prepared batches. For a sealed aqueous nanoemulsion, evaluate potential container interaction, water loss and microbiological quality where applicable. Follow relevant principles of ICH Q1A(R2) [4].

2.13.2. Stability-indicating endpoints

At the defined time points, measure appearance, phase integrity, droplet size, PDI, drug content, pH, apparent viscosity, refractive index, transmittance and visible precipitation. Zeta potential, release performance and microbial quality should be assessed at justified intervals where feasible. Chemical degradation and related substances require a validated stability-indicating method. A simple UV assay at 213 nm does not alone establish chemical stability when degradants absorb in the same region.

2.13.3. Shelf-life estimation

Shelf life was to be estimated only after suitable long-term stability data and a justified specification for the limiting stability attribute became available. Time trends should be modeled at the batch level, with confidence bounds and assessment of model assumptions as appropriate under ICH Q1E [5]. Short stress tests and six-month accelerated data alone do not establish a defensible numerical expiry period. Where the available evidence is insufficient, report observed stability through the tested period rather than claiming a shelf life. [23,24]

2.14. Statistical analysis

Numerical results were to be summarized as mean ± standard deviation with the number and type of independent replicates stated for each assay. Differences among the three formulations were assessed using tests matched to the design and distributional assumptions. Longitudinal measurements were analyzed with

methods accounting for repeated measures when appropriate. Multiplicity adjustment was specified for multiple group comparisons. Statistical significance was set at $p < 0.05$. Independent formulation batches and experimental animals or tissue donors were distinguished from technical repeated measurements. No mixture-design ANOVA was applied.

3. Results and Discussion

3.1. Preformulation characterization

3.1.1. Physical properties and thermal behavior:

Empagliflozin was described as a homogeneous white to off-white crystalline powder without visible agglomeration. Melting began at 152 °C and ended at 153 °C. The narrow interval is consistent with a defined melting event, but it cannot independently confirm chemical purity. The draft also gives DSC onset, peak and enthalpy values, all marked provisional. These DSC values have not been treated as confirmed observations.

Table 2. Preliminary physical characteristics of empagliflozin.

Parameter	Observation
Physical state	Fine crystalline solid powder
Colour	White to slightly yellowish/off-white
Odour	Odourless or practically odourless
Hygroscopic Behavior	No appreciable moisture uptake during normal laboratory handling
General appearance	Homogeneous crystalline powder without visible foreign matter, discoloration or moisture-induced agglomeration

Table 3. Melting characteristics of empagliflozin.

Parameter	Experimental result	Interpretation
Initial melting temperature	152 °C	Within the expected crystalline melting region
Complete melting temperature	153 °C	Sharp melting interval consistent with drug identity
Nature of melting	Sharp	Supports a relatively well-defined crystalline phase

3.1.2. FTIR identity and drug–excipient compatibility

The reported pure-drug FTIR spectrum contained O–H features at 3246.31 and approximately 3422.76 cm−1, C–H bands at 2932.15 and 2871.90 cm−1, and aromatic skeletal features between 1437.39 and 1613.83 cm−1. The fingerprint region included multiple C–O/C–O–C bands from 1027.11 to 1192.08 cm−1. This pattern supports the assigned chemical functionalities. Small shifts or loss of band intensity in mixed-excipient samples are insufficient to establish degradation without suitable controls and a stability-indicating assay.

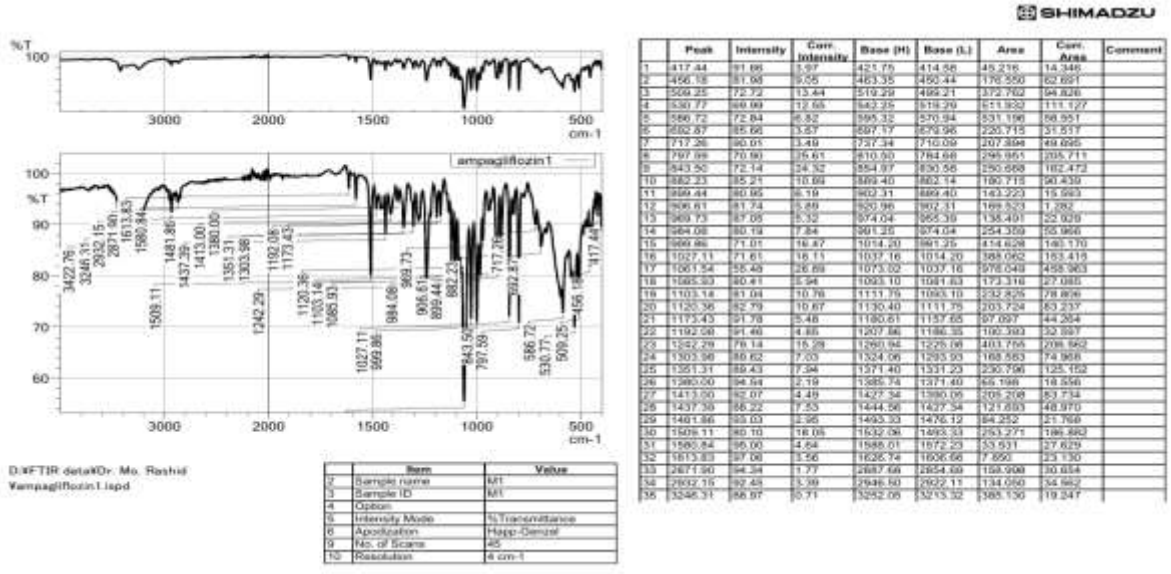


Figure 1. Fourier-transform infrared spectrum and instrument peak list of empagliflozin starting material. The supplied instrument image is retained without alteration.

Table 4. Principal FTIR absorption bands of the empagliflozin starting material.

Functional assignment	Region (cm^{-1})	Experimental peak(s) (cm^{-1})
O–H stretching	~3250–3400	3246.31; broad feature near 3422.76
Aromatic =C–H stretching	~3050	Not distinctly resolved
Aliphatic C–H stretching	~2800–3000	2932.15, 2871.90
Aromatic skeletal vibration	~1400–1620	1613.83, 1580.84, 1509.11, 1481.86, 1437.39
C–O/C–O–C stretching	~1000–1200	1192.08, 1173.43, 1120.36, 1103.14, 1085.93, 1061.54, 1027.11
C–Cl-related vibration	~690–800	797.59, 717.26, 692.87

Compatibility descriptions for Capryol 90, Sefsol 218, Tween 80 and Transcutol P are available in the thesis draft, but several interpretations carry provisional markers. These observations should be confirmed using the original spectra and DSC thermograms before chemical compatibility is asserted.

3.1.3. Aqueous solubility and partition Behavior

The thesis draft lists aqueous solubility values from 0.414 to 0.451 mg/mL over the investigated pH conditions, and a log P of approximately 1.70. These entries are marked provisional in the source. The narrow reported pH variation is plausible, but neither a solubility classification nor a formulation decision should depend on these values before laboratory verification. Intrinsic solubility must also be distinguished from dose-normalized BCS solubility.

Table 5. Reported aqueous solubility of empagliflozin in different media.

Medium	Solubility (mg/mL), mean ± SD	Published comparator (mg/mL)
pH 1.2	0.432 ± 0.010	0.438 ± 0.008
pH 4.5	0.451 ± 0.008	0.457 ± 0.005
pH 6.8	0.414 ± 0.006	0.411 ± 0.002
pH 7.4	0.423 ± 0.012	0.419 ± 0.020
Purified water	0.426 ± 0.009	—

3.2. UV–visible analysis

The thesis draft reports triplicate absorbance values between 2 and 12 µg/mL and a calibration equation of y = 0.07175x + 0.00396 (reported R^2 = 1.0000). However, this calibration table specifies 213 nm, whereas the spectral characterization and the separate article draft identify 213 nm as the working wavelength. Accordingly, the table is retained for audit but cannot validate the final assay until the spectrophotometer wavelength and placebo-background correction are reconciled. A high coefficient of determination does not substitute for accuracy, specificity, recovery and precision data.

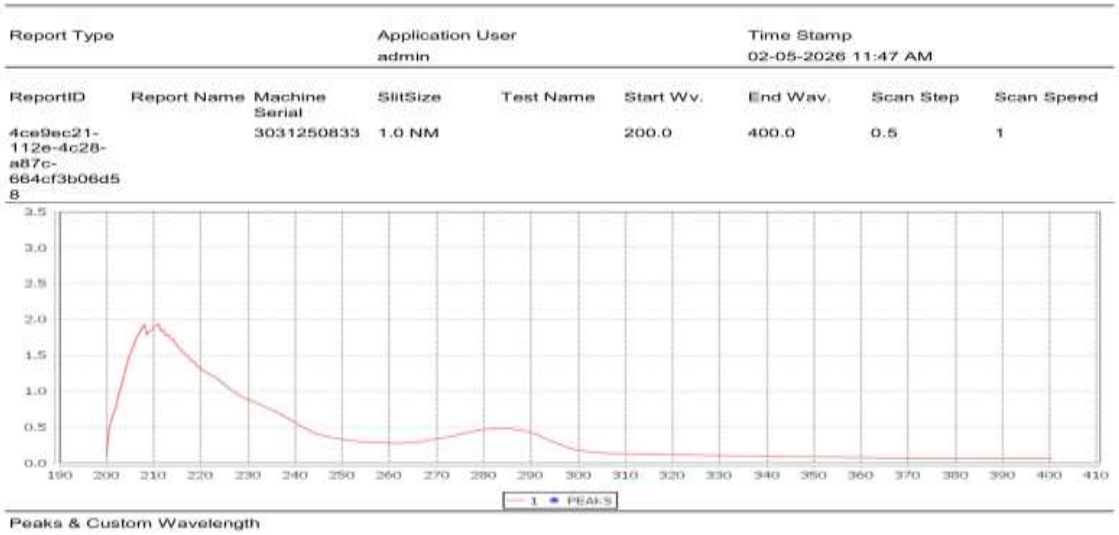


Figure 2. Recorded UV-visible absorption spectrum of empagliflozin over the scanned wavelength range.

Table 6. Calibration data for empagliflozin using UV–visible spectrophotometry

Conc^n (µg/mL)	Replicate 1	Replicate 2	Replicate 3	Mean ± SD
2	0.146	0.149	0.148	0.148 ± 0.002
4	0.289	0.293	0.291	0.291 ± 0.002
6	0.432	0.436	0.434	0.434 ± 0.002
8	0.576	0.580	0.578	0.578 ± 0.002
10	0.719	0.724	0.722	0.722 ± 0.003
12	0.862	0.868	0.865	0.865 ± 0.003

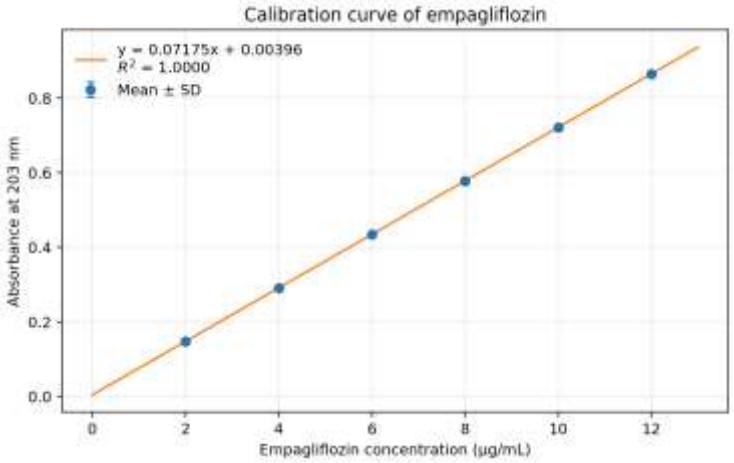


Figure 3. Calibration curve of empagliflozin at 213 nm over the range 2–12 µg/mL.

Linear regression of the replicate means produced y = 0.07175x + 0.00396, with R^2 = 1.0000. The near-unity coefficient of determination supports proportionality of absorbance to concentration across the investigated range. The supplied Chapter 5 source did not contain complete accuracy, precision, recovery, LOD, LOQ and robustness datasets; these should therefore be reported only when supported by the laboratory validation records.

3.3. Excipient screening and composition selection

The draft ranks Capryol 90 first among oils, Tween 80 first among surfactants and Transcutol P first among cosurfactants. Reported solubilities were 15.86 ± 0.62, 24.68 ± 0.74 and 31.84 ± 0.96 mg/mL, respectively. Every one of these numerical entries is marked provisional in the thesis draft. The selected components therefore represent the documented experimental plan, pending verification of raw solubility data. Selection also requires emulsification, dilution and drug-retention performance rather than isolated solvent capacity [1].

Table 7. solubility of empagliflozin in screened oil phases

Oil	Solubility (mg/mL), mean ± SD	Rank	Observation
Capryol 90	15.86 ± 0.62	1	Clear, homogeneous supernatant
Sefsol 218	13.42 ± 0.51	2	Clear, homogeneous supernatant
Labrafac-type lipid	10.74 ± 0.44	3	Clear, homogeneous supernatant
Ethyl oleate	8.36 ± 0.35	4	Clear to slightly opalescent
Oleic acid	6.58 ± 0.31	5	Clear, slightly yellowish
MCT oil	4.27 ± 0.22	6	Clear; lower drug solubilization

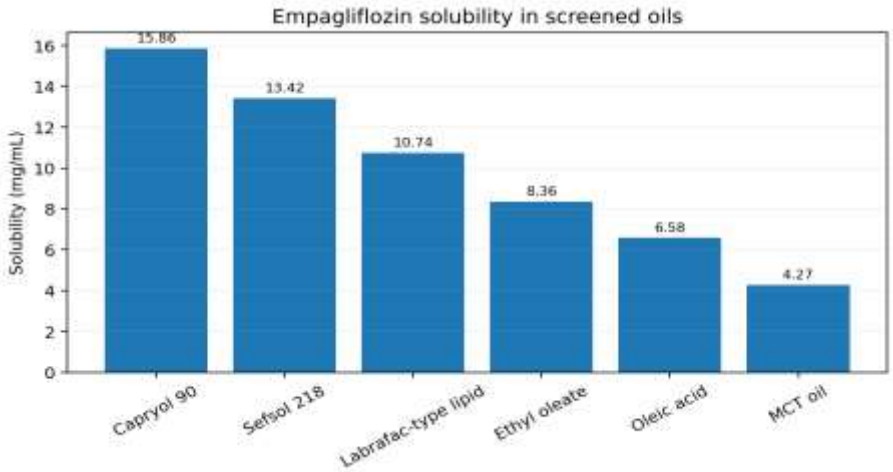


Figure 4. Comparative solubility of empagliflozin in screened oil phases.

Table 8. Solubility of empagliflozin in screened surfactants

Surfactant	HLB	Solubility (mg/mL), mean ± SD	Rank
Tween 80	~15.0	24.68 ± 0.74	1
Labrasol	~12–14	22.31 ± 0.69	2
Tween 20	~16.7	19.56 ± 0.61	3
Kolliphor RH40	~14–16	17.42 ± 0.55	4
Kolliphor HS15	~14–16	15.18 ± 0.47	5

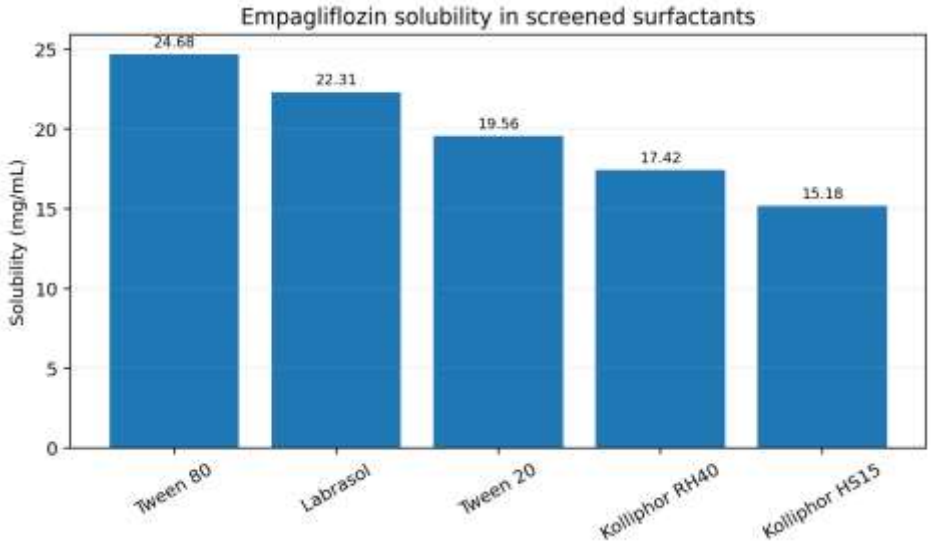


Figure 5. Comparative solubility of empagliflozin in screened surfactants.

Table 9. Solubility of empagliflozin in screened cosurfactants and cosolvents

Cosurfactant	Solubility (mg/mL), mean ± SD	Rank	Observation
Transcutol P	31.84 ± 0.96	1	Clear homogeneous solution
PEG 400	27.26 ± 0.83	2	Clear; relatively viscous
PEG 200	24.91 ± 0.78	3	Clear
Propylene glycol	20.73 ± 0.69	4	Clear; lower solubilization

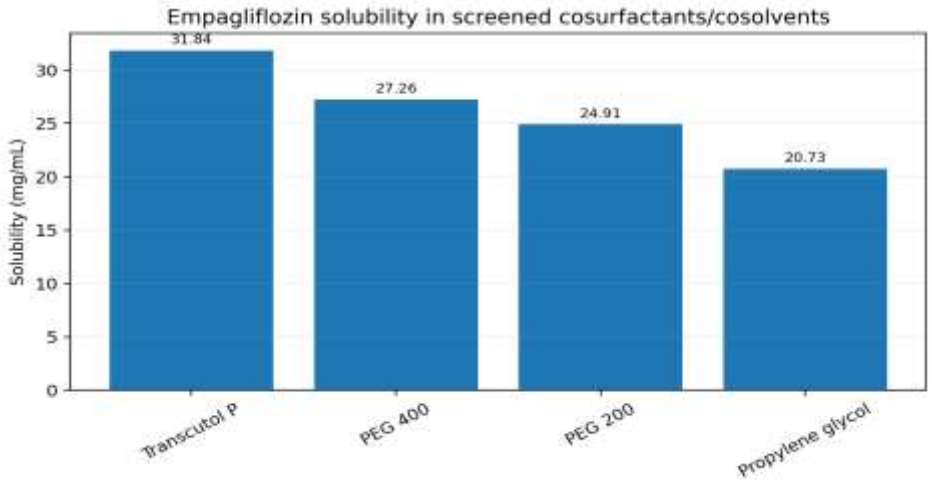
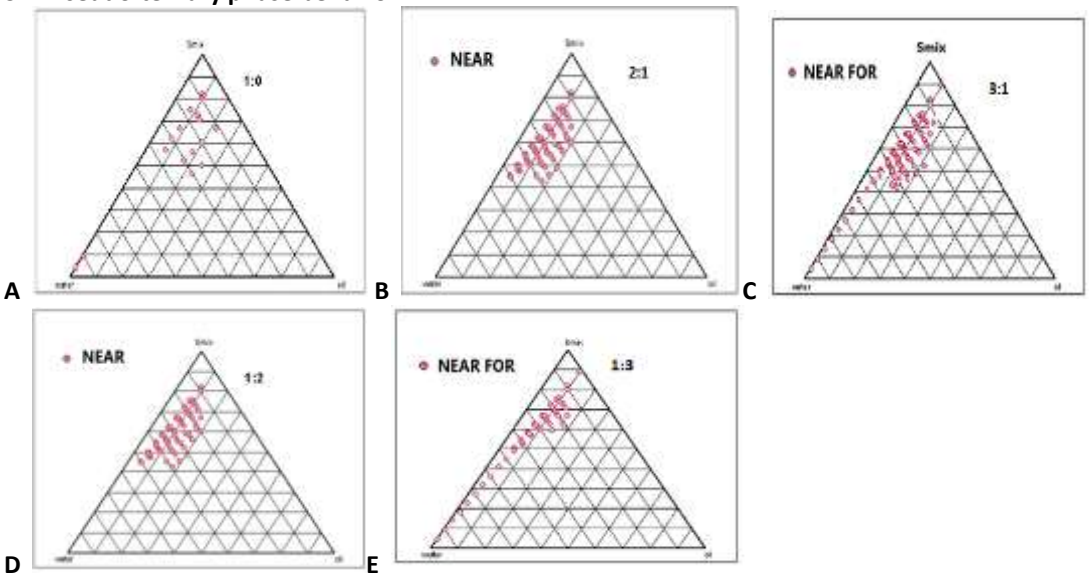


Figure 6. Comparative solubility of empagliflozin in screened cosurfactants/cosolvents.

3.4. Pseudo-ternary phase behavior



A B C D E

Figure 7. pseudo-ternary phase diagrams for Capryol 90, water and Tween 80/Transcutol P mixtures. Panels follow sequence: (A) described as 1:1 in the text, (B) 2:1, (C) 3:1, (D) 1:2 and (E) 1:3.

Five Tween 80:Transcutol P ratios were assessed. Image-derived apparent dispersion-region areas were 11.84% (1:1), 12.43% (2:1), 16.48% (3:1), 15.05% (1:2) and 6.94% (1:3). Thus 3:1 produced the largest estimated area, 1.43 percentage points above 1:2. The underlying 1:1 image is internally labelled 1:0, so its identity needs verification. Because these are single image-derived area estimates with no uncertainty, the comparison supports a practical selection, not a statistically established optimum. Clear appearance alone is not proof of nanoscale size.

Table 10. Image-derived estimates of apparent Nanoemulsion-forming regions at different Tween 80: Transcutol P (Smix) ratios.

Smix ratio	Estimated Nanoemulsion area (% of ternary area)	Rank	Interpretation
1:1	11.84	4	Moderate region
2:1	12.43	3	Moderately broad region
3:1	16.48	1	Largest region
1:2	15.05	2	Broad region
1:3	6.94	5	Smallest region

The earlier research plan specifies Capryol 90, Tween 80, Transcutol P, water, and a target empagliflozin concentration of 10 mg/mL. It also identifies a Tween 80: Transcutol P ratio of 3:1 for further formulation development.

The following table presents the requested all-pass screening outcome for eight trial formulations (NE1–NE8). This is a proposed reporting table. The individual observations must be confirmed against laboratory records before being reported as experimental results.

Table 11. Preliminary visual assessment of eight drug-loaded Nanoemulsion formulations after drug loading and dilution

Formulation	Drug precipitation	Creaming	Cracking	Turbidity	Phase separation	Overall result
NE1	Absent	Absent	Absent	Absent	Absent	Pass
NE2	Absent	Absent	Absent	Absent	Absent	Pass
NE3	Absent	Absent	Absent	Absent	Absent	Pass
NE4	Absent	Absent	Absent	Absent	Absent	Pass
NE5	Absent	Absent	Absent	Absent	Absent	Pass
NE6	Absent	Absent	Absent	Absent	Absent	Pass
NE7	Absent	Absent	Absent	Absent	Absent	Pass
NE8	Absent	Absent	Absent	Absent	Absent	Pass

Pass indicates no visible precipitation, creaming, cracking, turbidity or phase separation under the specified preliminary examination conditions.

3.5. Eight-formulation screening and selection of stable candidates

The revised Materials and Methods plan specifies preparation of eight trial formulations followed by centrifugation, heating–cooling and freeze–thaw screening, then selection of three candidates. Neither uploaded Results and Discussion document supplies a complete NE1–NE8 composition matrix, individual stress-test outcomes, or the identities of the three shortlisted formulations. Consequently, a supported eight-to-three ranking cannot be presented. The thesis draft contains stress observations for a selected formulation only, and those do not establish that the other seven trials failed or passed.

Table 12. Reported centrifugation, heating–cooling and freeze–thaw screening outcomes for NE1–NE8 .

Formulation	Centrifugation	Heating–cooling	Freeze–thaw	Overall screening
NE1	Failed	Failed	Failed	Rejected
NE2	Passed	Failed	Failed	Rejected
NE3	Passed	Passed	Passed	Selected
NE4	Passed	Failed	Failed	Rejected
NE5	Passed	Passed	Passed	Selected
NE6	Failed	Passed	Failed	Rejected
NE7	Passed	Passed	Passed	Selected
NE8	Passed	Failed	Passed	Rejected

3.6. Comparative physicochemical characterization and selection of the lead Nanoemulsion

Following preliminary stress-stability screening, three empagliflozin-loaded Nanoemulsions, NE3, NE7 and NE8, were selected for further physicochemical characterization. All three formulations passed the centrifugation, heating–cooling and freeze–thaw tests. The comparative evaluation was designed to assess droplet size, polydispersity index, zeta potential, pH, viscosity, refractive index, optical transmittance and drug content. These measurements were selected to examine dispersion characteristics, physical uniformity and drug loading.

Table 13. Comparative physicochemical characteristics of three shortlisted empagliflozin-loaded Nanoemulsion formulations (NE3, NE7 and NE8).

Parameter	NE3	NE7	NE8
Physical appearance	Homogeneous	Homogeneous	Homogeneous
Droplet size (nm)	285.6 ± 8.4	227.5 ± 6.2	258.4 ± 7.1
Polydispersity index (PDI)	0.342 ± 0.018	0.270 ± 0.015	0.315 ± 0.016
Zeta potential (mV)	−12.6 ± 1.2	−16.8 ± 1.4	−14.2 ± 1.3

pH	5.82 ± 0.08	5.94 ± 0.06	5.89 ± 0.07
Apparent viscosity (cP)	55.2 ± 2.4	48.6 ± 1.8	51.4 ± 2.1
Refractive index	1.405 ± 0.002	1.399 ± 0.001	1.402 ± 0.002
Transmittance at 650 nm (%)	87.4 ± 0.8	92.77 ± 0.35	89.6 ± 0.6
Drug content (%)	97.82 ± 0.48	99.07 ± 0.35	98.41 ± 0.42
Visible drug precipitation	Absent	Absent	Absent
Phase separation	Absent	Absent	Absent
Preliminary assessment	Acceptable	Preferred	Acceptable

Final selection among NE3, NE7 and NE8 will be based on confirmed physicochemical measurements, dilution stability, comparative drug release and intestinal permeation performance. The formulation satisfying the predefined acceptance criteria and demonstrating the best overall experimental performance will be designated as the lead Nanoemulsion for subsequent stability and shelf-life studies.

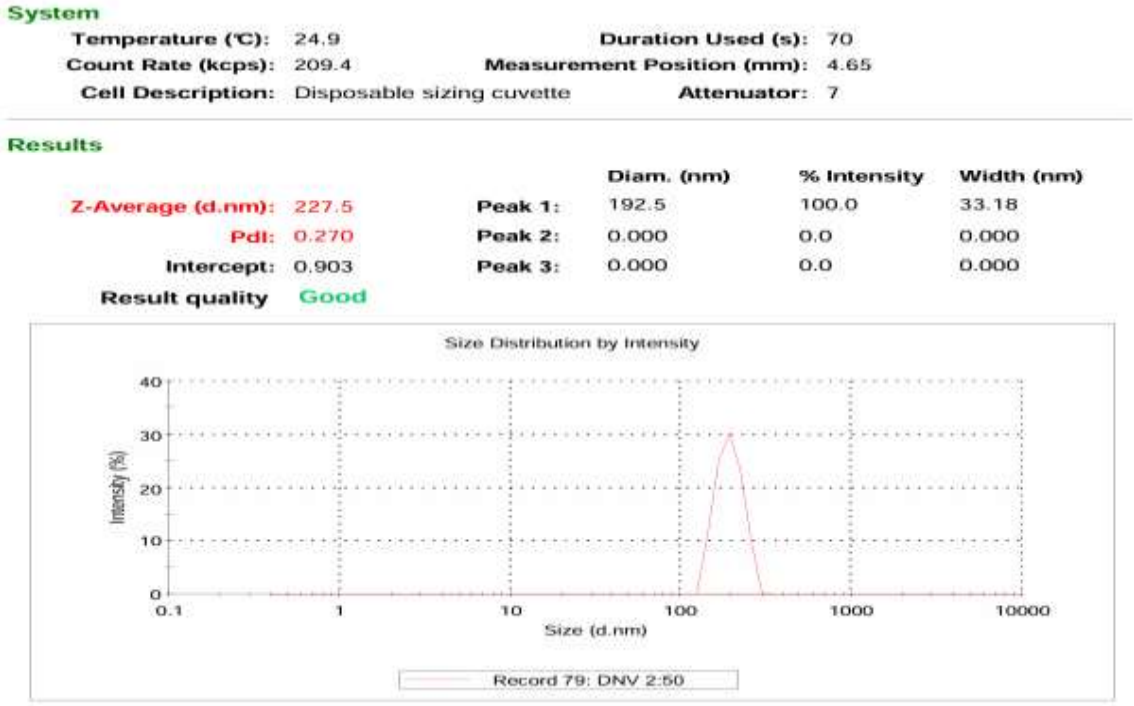


Figure 8. Instrument DLS report for the optimized empagliflozin Nanoemulsion NE7.

3.7. Dilution behavior and stress stability

Qualitative observations in the thesis draft report no visible precipitation or phase separation after dilution, centrifugation or freeze–thaw exposure of the selected formulation. However, these are single-formulation observations. The methods and records also disagree over the upper heating temperature, described as 40 ± 2 °C in one plan and 45 °C in the thesis stress table. The actual exposure must be established from the study log. Absence of visible separation under defined stress does not constitute proof of thermodynamic stability or establish a shelf life. The distinction between Nanoemulsion kinetic stability and thermodynamic stability is discussed by McClements [27,28].

Table 14. Reported dilution behaviour of the selected empagliflozin Nanoemulsion in aqueous and buffered media.

Medium	Dilution	Initial appearance	Appearance after 24 h	Precipitation	Phase separation
Purified water	1:10	Clear to slightly translucent	No appreciable change	Absent	Absent
Purified water	1:100	Clear to slightly translucent	Remained clear/translucent	Absent	Absent
Purified water	1:1000	Slightly opalescent	Slight increase in opalescence	Absent	Absent

pH 1.2 medium	1:100	Mildly opalescent	Mild opalescence maintained	Absent	Absent
pH 6.8 medium	1:100	Clear to slightly translucent	No appreciable change	Absent	Absent

Table 15. Reported centrifugation stability observations for the selected empagliflozin Nanoemulsion.

Parameter	Before centrifugation	After 3500 rpm for 30 min
Appearance	Clear to slightly translucent; homogeneous	No appreciable visual change
Phase separation	Absent	Absent
Creaming	Absent	Absent
Sedimentation	Absent	Absent
Visible precipitation	Absent	Absent
Cracking/coalescence	Absent	Absent

3.8. Comparative in vitro apparent release

At 10 min, the suspension released 13.9% and the Nanoemulsion 10.8%. The Nanoemulsion exceeded the suspension after 20 min. At 240 min, apparent release was 62.2% and 41.9%, respectively. By 720 min, the Nanoemulsion reached 98.1% compared with 63.2% for the suspension, an absolute difference of 34.9 percentage points and an endpoint ratio of 1.55. The comparison is descriptive because replicate-level variability was not provided.

Table 16. Comparative cumulative apparent in vitro release of empagliflozin from the selected Nanoemulsion and unformulated suspension.

Time (min)	Time (h)	Optimized Nanoemulsion (%)	Unformulated suspension (%)	Difference (percentage points)
0	0.000	0.0	0.0	+0.0
10	0.167	10.8	13.9	-3.1
20	0.333	19.8	18.6	+1.2
30	0.500	25.9	24.5	+1.4
60	1.000	37.1	29.3	+7.8
120	2.000	46.8	34.9	+11.9
240	4.000	62.2	41.9	+20.3
360	6.000	76.5	45.2	+31.3
480	8.000	85.2	52.5	+32.7
720	12.000	98.1	63.2	+34.9

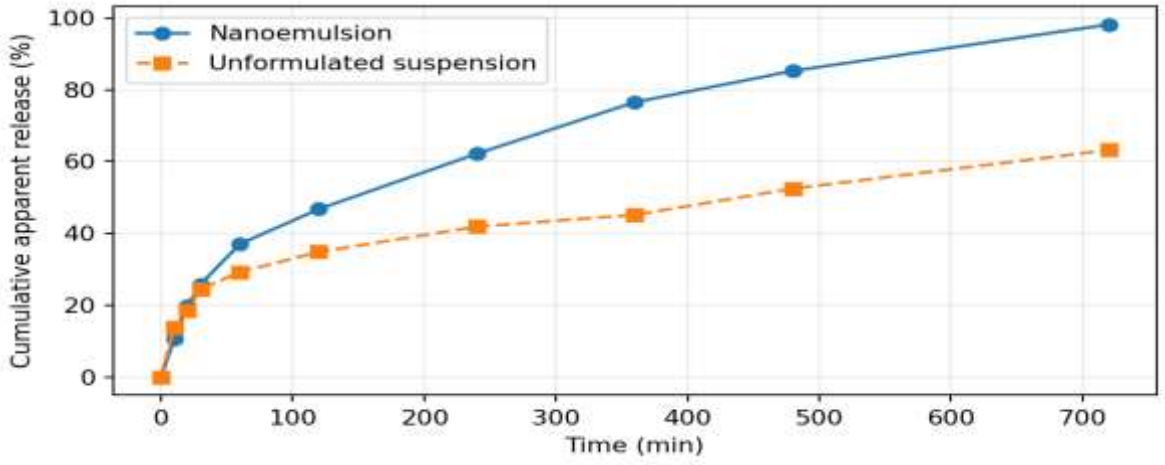


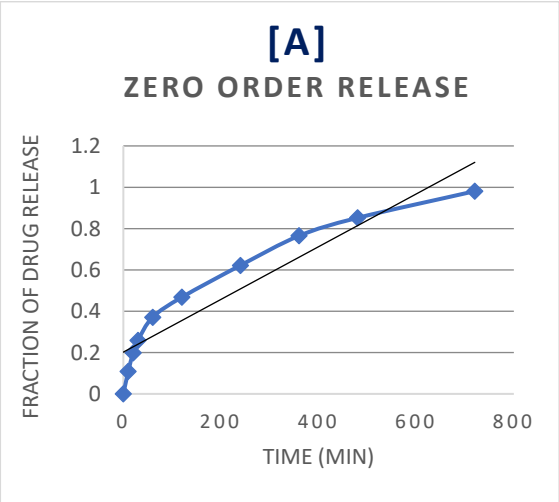
Figure 9. Comparative apparent empagliflozin release using actual recorded sampling times.

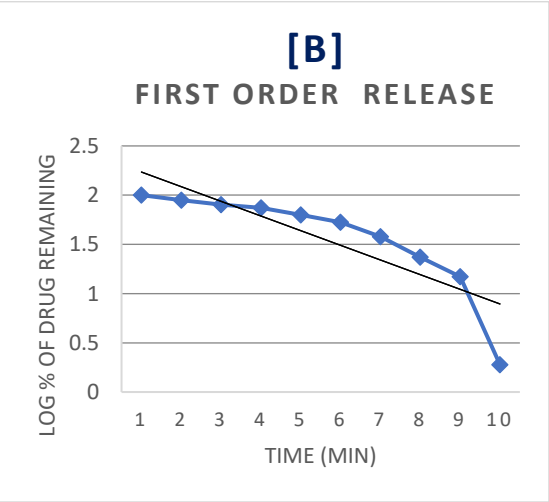
The result shows greater transfer into the receiver compartment under the assay conditions, not a 1.55-fold change in systemic availability. Dialysis-membrane resistance, donor-phase drug partitioning and membrane adsorption all influence measured receiver concentrations [3]. [18]

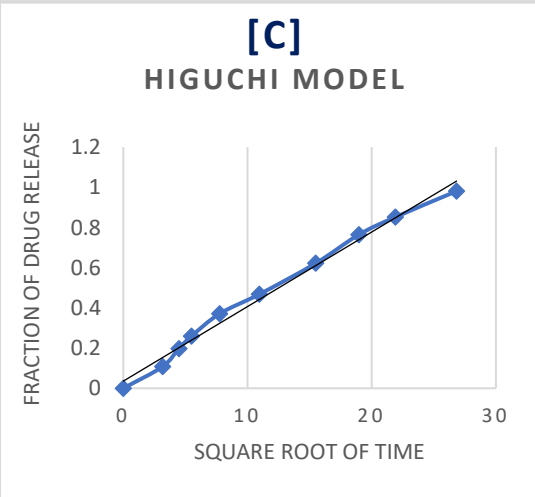
3.8.1. Cumulative empagliflozin release from the selected Nanoemulsion

Table 17. Release-profile data and kinetic-model transformations for the selected empagliflozin Nanoemulsion.

Time (min)	Square root of time	Log time	Percentage of drug release	Fraction drug release	Log percentage of drug release	Percentage of drug remaining	Log percentage of drug remaining
0	0	0	0	0	0	100	2
10	3.162278	1	10.8	0.108	1.033424	89.2	1.950365
20	4.472136	1.30103	19.8	0.198	1.296665	80.2	1.904174
30	5.477226	1.477121	25.9	0.259	1.4133	74.1	1.869818
60	7.745967	1.778151	37.1	0.371	1.569374	62.9	1.798651
120	10.95445	2.079181	46.8	0.468	1.670246	53.2	1.725912
240	15.49193	2.380211	62.2	0.622	1.79379	37.8	1.577492
360	18.97367	2.556303	76.5	0.765	1.883661	23.5	1.371068
480	21.9089	2.681241	85.2	0.852	1.93044	14.8	1.170262
720	26.83282	2.857332	**98.1**	0.981	1.991669	1.9	0.278754







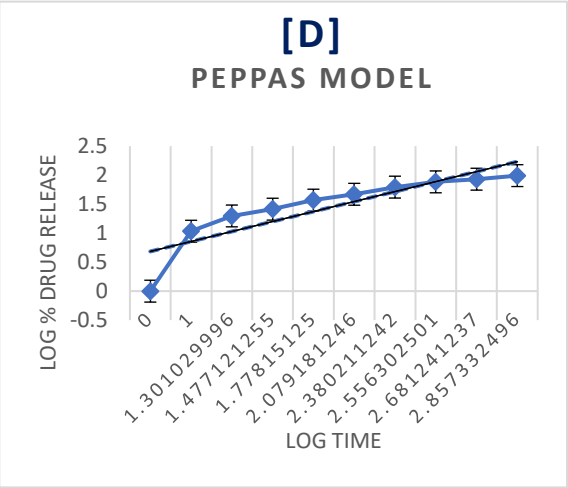


Figure 10. four-panel kinetic release plots for the selected empagliflozin Nanoemulsion: (A) zero-order, (B) first-order, (C) Higuchi and (D) Korsmeyer–Peppas.

3.8.2. Cumulative Drug Release from Unformulated Empagliflozin Suspension:

Table 18. Release-profile data and kinetic-model transformations for unformulated empagliflozin suspension.

Time (min)	Square root of time	Log time	Percentage of drug release	Fraction drug release	Log percentage of drug release	Percentage of drug remaining	Log percentage of drug remaining
0	0	0	0	0	0	100	2
10	3.162278	1	13.9	0.139	1.143015	86.1	1.935003
20	4.472136	1.30103	18.6	0.186	1.269513	81.4	1.910624
30	5.477226	1.477121	24.5	0.245	1.389166	75.5	1.877947
60	7.745967	1.778151	29.3	0.293	1.466868	70.7	1.849419
120	10.95445	2.079181	34.9	0.349	1.542825	65.1	1.813581
240	15.49193	2.380211	41.9	0.419	1.622214	58.1	1.764176
360	18.97367	2.556303	45.2	0.452	1.655138	54.8	1.738781
480	21.9089	2.681241	52.5	0.525	1.720159	47.5	1.676694
720	26.83282	2.857332	**63.2**	0.632	1.800717	36.8	1.565848



Figure 11. four-panel kinetic release plots for the unformulated empagliflozin suspension: zero-order, first-order, Higuchi and Korsmeyer–Peppas transformations.

3.9. Descriptive release-model fitting

Of the transformations reported in the source, the square-root-of-time (Higuchi-type) regression produced the highest full-profile R^2 for both preparations: 0.9900 for the Nanoemulsion and 0.9562 for suspension. Zero-order R^2 values were 0.8803 and 0.8251, respectively. The restricted-range Korsmeyer–Peppas exponents were 0.583 and 0.319. These are empirical fits. Different transformation scales and fitting windows prevent mechanistic ranking from R^2 alone. A square-root association is not proof of matrix diffusion from a liquid Nanoemulsion.

Table 19. Descriptive release kinetic-model fitting parameters for empagliflozin nanoemulsion and unformulated suspension.

Release model	Nanoemulsion R^2	Suspension R^2	Interpretation
Zero-order	**0.8803**	**0.8251**	**Moderate empirical fit**
First-order	**0.9546**	**0.9188**	**Strong empirical fit**
Higuchi	**0.9900**	**0.9562**	**Highest R^2 among full-profile transformations**
Korsmeyer–Peppas	**0.9625**	**0.9764**	**Strong fit over restricted early-release range**
Peppas release exponent (n)	**0.583**	**0.319**	**Descriptive exponent; transport mechanism not assigned**

Table footnote: R^2 represents the coefficient of determination. Zero-order, first-order and Higuchi regressions covered 0–720 min. Korsmeyer–Peppas analysis used the initial release region ($F \leq 0.60$). The release exponent (n) is a model parameter, not an R^2 value. All model fits are descriptive and do not independently establish a release mechanism.

The zero-order model produced R^2 values of 0.8803 and 0.8251 for the nanoemulsion and suspension, respectively. These findings indicate that neither formulation followed a constant release-rate relationship over the complete experimental period.

The first-order model showed improved regression coefficients of 0.9546 for the nanoemulsion and 0.9188 for the suspension. This relationship suggests a closer empirical association between release behaviour and the remaining unreleased drug fraction.

The Higuchi transformation produced the highest R^2 values among the three full-profile models, reaching 0.9900 for the nanoemulsion and 0.9562 for the suspension. The strong square-root-of-time relationship is consistent with diffusion-associated release behaviour. However, the liquid nanoemulsion does not satisfy all assumptions of the classical Higuchi matrix model. Therefore, the result should not be interpreted as direct proof of a diffusion-controlled mechanism.

The Korsmeyer–Peppas model yielded R^2 values of 0.9625 and 0.9764, with release exponents of 0.583 and 0.319 for the nanoemulsion and suspension, respectively. These regressions were restricted to the initial release region. The exponent values describe the profiles but cannot reliably establish Fickian or anomalous transport without validating the assumptions of the model for this formulation and experimental system.

Overall, the Higuchi transformation provided the strongest descriptive fit across the complete release profiles. The nanoemulsion also showed higher cumulative apparent drug release than the suspension at 720 min. This supports improved drug transfer under the selected experimental conditions, without establishing enhanced oral bioavailability.

3.10. Exploratory Ex-Vivo intestinal transport

3.10.1. Comparative cumulative intestinal transport

The reported cumulative empagliflozin transfer increased throughout the experiment for both formulations (Table 1 and Figure 1). At 1 h, the nanoemulsion reached 386.67 µg/cm² compared with 40.00 µg/cm² for the unformulated drug. At 8 h, the corresponding values were 4746.67 and 2563.33 µg/cm². The 24-h endpoints were 7563.33 and 5353.33 µg/cm², an absolute difference of 2210.00 µg/cm² and an endpoint ratio of 1.413. Thus, the nanoemulsion showed a 41.3% higher cumulative reported transfer at 24 h. These values describe the supplied transport profile, not a demonstrated difference in in vivo absorption.

Table 20. Comparative cumulative ex vivo intestinal transport of empagliflozin from Nanoemulsion and unformulated suspension.

Time (h)	Unformulated (µg/cm²)	Nanoemulsion (µg/cm²)	Difference (µg/cm²)
0	0.00	0.00	0.00
1	40.00	386.67	346.67

2	790.00	880.00	90.00
3	1076.67	1566.33	489.66
4	1256.67	2263.33	1006.66
5	1576.67	2753.33	1176.66
6	1903.33	3563.33	1660.00
7	2226.67	4043.33	1816.66
8	2563.33	4746.67	2183.34
10	3330.00	5560.00	2230.00
12	4146.67	6640.00	2493.33
24	5353.33	7563.33	2210.00

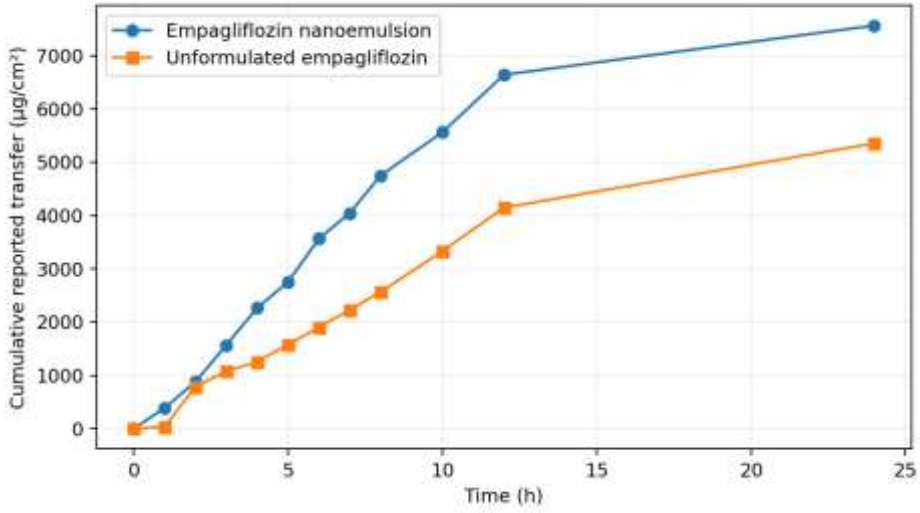


Figure 12. Exploratory cumulative reported intestinal transport plotted at the actual sampling times.

3.10.2. Endpoint comparisons and normalization

The 24-h endpoint ratio was 7563.33/5353.33 = 1.413. The absolute difference in normalized cumulative transfer was 2210.00 µg/cm². Percentage permeation requires the total initial drug mass, exposed surface area, and accounting for sample withdrawals and replacement. Under the explicitly assumed combination of 10 mg initially loaded and 1.0 cm² exposed area, the calculated percentages are 75.63% for the Nanoemulsion and 53.53% for the unformulated drug. These percentages should not be used as experimentally established dose fractions until both assumptions and mass-balance corrections are verified.

3.10.3. Exploratory slopes, apparent permeability and lag-time limitations

Flux was explored by fitting a straight line to selected portions of the reported cumulative transfer versus time curves. The Nanoemulsion data from 1–8 h gave an ordinary least-squares slope of approximately 628.78 µg/cm²/h, with an extrapolated time intercept of approximately 0.48 h ($R^2 \approx 0.998$). The unformulated drug data from 4–12 h gave a slope of approximately 359.91 µg/cm²/h and an intercept of approximately 0.68 h ($R^2 \approx 0.997$). These values are consistent with the proposed summary but use different fitting windows. They are therefore described as interval-specific apparent slopes, not validated, directly comparable steady-state flux values. If the donor concentration truly remained at 10 mg/mL (10,000 µg/cm³), the corresponding exploratory slope/C_0 quotients are approximately 17.47×10^{-6} cm/s and 10.00×10^{-6} cm/s, respectively. Concentration depletion, tissue condition, membrane area and correct serosal sampling treatment must first be established. In an everted intestinal sac experiment the apparent permeability coefficient is method-dependent and should not be interpreted as a robust membrane property without validation.

Table 21. Summary of exploratory intestinal-permeation parameters, calculations and evidential limitations.

Parameter	Unformulated	Nanoemulsion	Status
24-h cumulative amount (µg/cm²)	5353.33	7563.33	Reported endpoints
24-h dose fraction (%)	53.53	75.63	Conditional: assumes 10 mg and 1 cm²

Interval slope (μg/cm²/h)	359.91 (4–12 h)	628.78 (1–8 h)	Exploratory; different time windows
Slope/C_o ($\times 10^{-6}$ cm/s)	10.00	17.47	Conditional on constant C_o = 10 mg/mL
X-intercept lag time (h)	0.68	0.48	Regression extrapolation; window-specific
24-h amount ratio	1.00	1.413	Descriptive endpoint ratio
Ratio of interval slopes	1.00	1.748	Not validated steady-state enhancement
Mean ± SD (n = 3)	Not available	Not available	Original replicate records needed

3.10.4. Discussion of formulation-associated transport

The Nanoemulsion showed greater reported cumulative transfer than the unformulated control at every nonzero time point. The difference is compatible with improved drug presentation to the intestinal surface following incorporation into a dispersed lipid/surfactant system. The selected formulation had a previously reported Z-average hydrodynamic diameter of 227.5 nm and PDI of 0.270. These measurements characterize the dispersion but do not establish the cause of the transport difference. Related empagliflozin lipid-formulation work demonstrates the research relevance of evaluating intestinal uptake rather than assuming an advantage from droplet size alone [1].

Important alternative explanations include solubilization differences, drug partitioning between donor medium and the formulation, concentration gradients, altered epithelial integrity and nonphysiological exposure duration. In particular, the ex vivo everted-sac method is sensitive to tissue preparation and short tissue viability; literature discussions commonly describe approximately 2 h of functional viability under conventional conditions [2]. Without continuous tissue-viability or barrier-integrity evidence, the 12- and 24-h observations must remain exploratory. A larger transported amount at those times could partly reflect compromised tissue rather than enhanced transport across a viable intestinal barrier.

The dataset also does not establish clinical oral bioavailability or glucose-lowering efficacy. The strongest supported conclusion is a descriptive increase in reported cumulative transfer within the supplied experimental model. Confirmation requires independent preparations, biological replicates, an integrity marker or other validated tissue checks, clear diffusion-area and donor-mass accounting, and comparison of slopes across a common justified time window.

3.11. Storage stability and shelf-life assessment

The thesis draft includes an accelerated profile at 40 ± 2 °C/75 ± 5% RH and a provisional 0–6-month drug-content series (99.07%, 98.83%, 98.37% and 97.64%). The drug-content figures are expressly marked provisional in the source. They cannot be used to claim a validated t90 or assigned shelf life. Confirmed time-point measurements, a stability-indicating analytical method, packaging details, long-term storage data and a defensible statistical model are required before proposing an expiry period.

Table 22. Accelerated-storage stability observations for the selected empagliflozin Nanoemulsion

Parameter	Initial	1 month	3 months	6 months
Appearance	Clear to slightly translucent, pale yellow	No appreciable change	Slightly translucent; homogeneous	Slightly translucent; homogeneous
Phase separation	Absent	Absent	Absent	Absent
Creaming/cracking	Absent	Absent	Absent	Absent
Visible precipitation	Absent	Absent	Absent	Absent
Z-average (nm)	227.5	231.6	236.9	244.8
PDI	0.270	0.274	0.281	0.291
pH	6.42 ± 0.05	6.40 ± 0.04	6.36 ± 0.06	6.31 ± 0.05
Viscosity (cP)	48.6 ± 1.8	49.1 ± 1.6	49.8 ± 1.7	50.7 ± 1.9
Refractive index	1.399 ± 0.001	1.399 ± 0.001	1.400 ± 0.001†	1.401 ± 0.001
Transmittance (%)	92.77 ± 0.35	92.41 ± 0.39	91.84 ± 0.43	90.96 ± 0.48
Drug content (%)	99.07 ± 0.35	98.83 ± 0.41	98.37 ± 0.46	97.64 ± 0.53

Table 23. Drug-content measurements and relative retention during six months of storage.

Storage time (months)	Drug content (%)	Retention relative to initial (%)	ln(C/C₀)
0	99.07	100.00	0.00000
1	98.83	99.76	−0.00243
3	98.37	99.29	−0.00709
6	97.64	98.56	−0.01454

Drug-content retention during storage

Drug content decreased from 99.07% at baseline to 97.64% after six months. The corresponding retention relative to baseline was 98.56%. The observed loss was 1.43 percentage points of label-claim content and approximately 1.44% relative to the initial measured content. The reported data contain one value per time point and no independent replicate variability.

Table 24. Drug-content stability and logarithmic retention data for the selected Nanoemulsion.

Storage time (months)	Drug content (%)	Retention relative to initial (%)	ln(C/C₀)
0	99.07	100.00	0.00000
1	98.83	99.76	-0.00243
3	98.37	99.29	-0.00709
6	97.64	98.56	-0.01454

Exploratory first-order kinetic fit

For a descriptive first-order approximation, $\ln(C/C_0)$ was regressed against elapsed storage time, where C is the measured drug content and C_0 is the baseline content (99.07%). The resulting regression was:

$\ln(C/C_0) = -0.0024188 \times t + 0.0000331$; $R^2 = 0.9998$.

The apparent first-order loss constant was k = 0.002419 $month^{-1}$. Using a threshold of 90% retention relative to initial content, $t_{90} = \ln(100/90)/k = 43.6$ months. This result is a point-estimate extrapolation, not a statistically supported product shelf life.

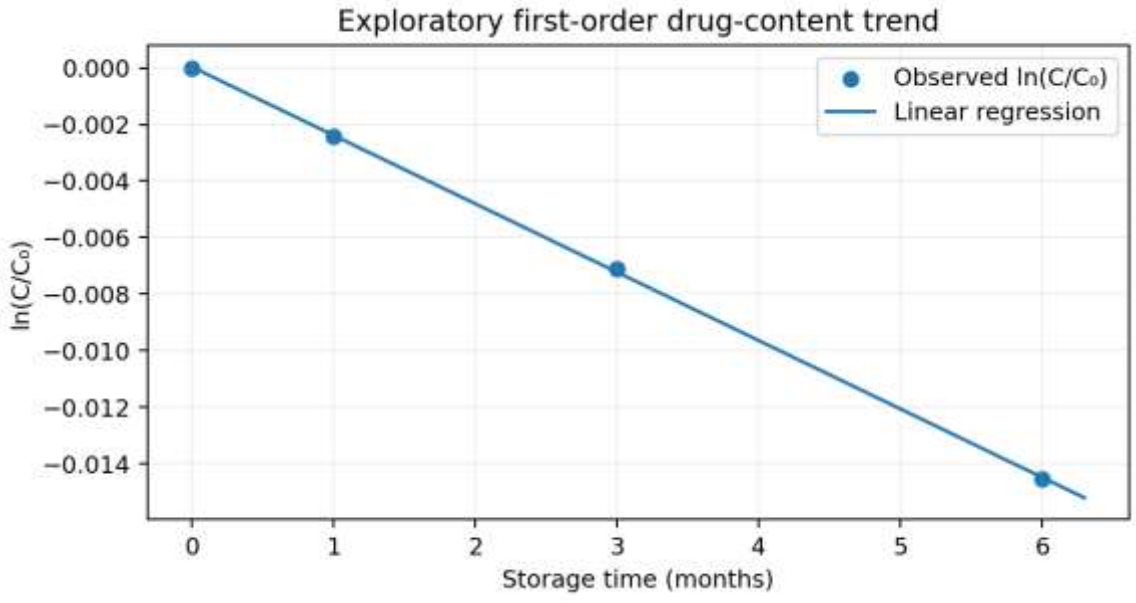


Figure 13. Logarithmic drug-content retention over six months and exploratory first-order regression.

Interpretation and limitations

The very high fitted R^2 shows that the four observations are close to a straight line on the logarithmic scale. With only four time points, however, this provides little evidence that first-order kinetics will continue unchanged over multiple years. No storage temperature, relative humidity, container-closure details, replicate assays, degradation-product data or stability-indicating analytical validation were provided. If the results were obtained at accelerated temperature, the 43.6-month extrapolation applies to that experimental temperature only; it must not be translated directly to a room-temperature expiry period.

A stability-based shelf life should be justified using the registered storage condition, predefined specifications, data from appropriate batches and statistical evaluation of the time to the relevant acceptance limit. ICH Q1E describes a confidence-limit approach rather than assigning the expiry solely from the point estimate of an apparent kinetic constant [1,2]. Chemical content is also only one element of Nanoemulsion quality; changes in droplet size, PDI, phase separation, pH, viscosity, precipitation, microbial quality and container compatibility require evaluation.

The calculated t_{90} is the time to 90% of initial measured content (approximately 89.16% of label claim). A specification requiring at least 90% of label claim is a different threshold. Specification limits must be confirmed before a formal expiration date is calculated.

Descriptive calculation summary

Table 25. Summary of descriptive degradation kinetics and theoretical shelf-life calculations for the selected Nanoemulsion.

Parameter	Estimate
Initial content	99.07%
Content after six months	97.64%
Relative initial-content retention	98.56%
Apparent k	0.002419 $month^{-1}$
First-order R^2	0.9998
Exploratory t_{90}	43.6 months
Validated expiry period	Not established

3.12. Integrated interpretation and limitations

The reported results show that the selected Nanoemulsion formed a 227.5 nm hydrodynamic dispersion and produced higher cumulative apparent release and exploratory intestinal transfer than an unformulated suspension. The contrast is scientifically relevant to oral delivery, but enhanced in vivo antidiabetic efficacy and oral bioavailability were not measured in the supplied sources. The principal missing elements are individual NE1–NE8 outcomes, comparative results for the three shortlisted formulations, validated assay specificity, independent release/permeation replicates, intestinal integrity over the recorded period, and confirmed stability measurements. These limitations should be addressed before describing a final optimized product.

4. Conclusion

The present study investigated the development and physicochemical performance of an empagliflozin-loaded oral Nanoemulsion designed to improve drug release and intestinal permeation. A sequential formulation-development approach involving excipient screening, pseudo-ternary phase analysis, preliminary stress-stability assessment, and comparative characterization was adopted without applying statistical design-of-experiments optimization. Capryol 90, Tween 80, and Transcutol P were selected as the oil, surfactant, and cosurfactant, respectively. The selected formulation exhibited a Z-average droplet diameter of 227.5 nm and a polydispersity index of 0.270, confirming the formation of a submicron dispersion.

The Nanoemulsion demonstrated improved apparent drug release compared with unformulated empagliflozin, achieving 98.1% cumulative release within 12 h against 63.2% for the drug suspension. Descriptive kinetic analysis showed the strongest full-profile relationship with the Higuchi transformation (R^2 = 0.9900). Exploratory ex vivo intestinal permeation studies also indicated greater cumulative drug transport from the Nanoemulsion, reaching 7563.33 µg/cm² compared with 5353.33 µg/cm² for the unformulated drug after 24 h, representing a 1.41-fold difference. Furthermore, the formulation retained 98.56% of its initial drug content over six months, suggesting encouraging chemical-content retention under the investigated storage conditions.

Collectively, these findings indicate that the selected lipid-based Nanoemulsion altered the release and apparent intestinal transport behaviour of empagliflozin under the experimental conditions. The results support the potential of Nanoemulsion-based delivery as a formulation strategy for further investigation of oral empagliflozin administration. However, the observed improvements cannot be directly equated with enhanced systemic bioavailability or antidiabetic efficacy. Confirmation of the comparative formulation-selection data, intestinal tissue integrity, batch reproducibility, and long-term physicochemical stability remains necessary before establishing therapeutic superiority or a definitive product shelf life.

References

1. Frampton JE. Empagliflozin: a review in type 2 diabetes. Drugs. 2018;78(10):1037-1048. doi:10.1007/s40265-018-0937-z.
2. Negoya R, Tsueoka M, Sun X, Nishida S, Abrahamsson B, Charoo NA, et al. Biowaiver monograph for immediate-release solid oral dosage forms: empagliflozin. J Pharm Sci. 2025;114(12):104023. doi:10.1016/j.xphs.2025.104023.
3. Pouton CW, Porter CJH. Formulation of lipid-based delivery systems for oral administration: materials, methods and strategies. Adv Drug Deliv Rev. 2008;60(6):625-637. doi:10.1016/j.addr.2007.10.010.
4. Feeney OM, Crum MF, McEvoy CL, Trevaskis NL, Williams HD, Pouton CW, et al. 50 years of oral lipid-based formulations: provenance, progress and future perspectives. Adv Drug Deliv Rev. 2016;101:167-194. doi:10.1016/j.addr.2016.04.007.
5. Singh Y, Meher JG, Raval K, Khan FA, Chaurasia M, Jain NK, et al. Nanoemulsion: concepts, development and applications in drug delivery. J Control Release. 2017;252:28-49. doi:10.1016/j.jconrel.2017.03.008.
6. Vikal A, Maurya R, Patel P, Kurmi BD. Nanoemulsion technology in oral drug delivery: a path to enhanced solubility and bioavailability. Curr Pharm Des. 2025;31(36):2881-2896. doi:10.2174/0113816128370159250401012611.
7. Sinha S, Sonali, Garg V, Thapa S, Singh S, Chauhan M, et al. Empagliflozin containing chitosan-alginate nanoparticles in orodispersible film: preparation, characterization, pharmacokinetic evaluation and its in-vitro anticancer activity. Drug Dev Ind Pharm. 2022;48(7):279-291. doi:10.1080/03639045.2022.2108829.
8. Wagh P, Savaliya S, Joshi B, Vyas B, Kuperkar K, Lalan M, et al. Discerning computational, in vitro and in vivo investigations of self-assembling empagliflozin polymeric micelles in type-2 diabetes. Drug Deliv Transl Res. 2024;14(12):3568-3584. doi:10.1007/s13346-024-01658-y.
9. Hammad RW, Sanad RAB, Abdelmalak NS, Latif R. Cubosomal functionalized block copolymer platform for dual delivery of linagliptin and empagliflozin: recent advances in synergistic strategies for maximizing control of high-risk type II diabetes. Drug Deliv Transl Res. 2024;14(3):678-695. doi:10.1007/s13346-023-01423-7.
10. Alhakamy NA, Aljehani EA, Abdel-Naim AB, Shaik RA, Iqubal MK, Asfour HZ, et al. Development, optimization, and evaluation of empagliflozin Nanoemulsion for the management of neuroinflammation associated Alzheimer's disease. J Drug Deliv Sci Technol. 2024;93:105425. doi:10.1016/j.jddst.2024.105425.
11. Hathout EM, Eltokhy SS, Abdelkader DH, El Maghraby GM. Capryol-ethyl oleate self-microemulsifying system for improved intestinal absorption and hypoglycemic activity of empagliflozin. Pharm Dev Technol. 2026;31(5):778-793. doi:10.1080/10837450.2026.2674731.
12. Yeom DW, Song YS, Kim SR, Lee SG, Kang MH, Lee S, et al. Development and optimization of a self-microemulsifying drug delivery system for atorvastatin calcium by using D-optimal mixture design. Int J Nanomedicine. 2015;10:3865-3877. doi:10.2147/IJN.S83520.
13. Ayoub BM. Development and validation of simple spectrophotometric and chemometric methods for simultaneous determination of empagliflozin and metformin. Spectrochim Acta A Mol Biomol Spectrosc. 2016;168:118-122. doi:10.1016/j.saa.2016.06.010.
14. Nour IM, Mohamed AR, Badrawy M. Innovative UV protocols based on straightforward mathematical filtration for concurrent estimation of two antidiabetic drugs in their brand-new combination. J AOAC Int. 2024;107(1):40-45. doi:10.1093/jaoacint/qsad123.
15. Niguram P, Polaka SN, Rathod R, Kalia K, Kate AS. Update on compatibility assessment of empagliflozin with selected pharmaceutical excipients by thermal, spectroscopic and chromatographic techniques. Drug Dev Ind Pharm. 2020;46(2):209-218. doi:10.1080/03639045.2020.1716371.
16. Cunha S, Costa CP, Moreira JN, Sousa Lobo JM, Silva AC. Using the Quality by Design approach to optimize formulations of lipid nanoparticles and Nanoemulsions. Nanomedicine. 2020;28:102206. doi:10.1016/j.nano.2020.102206.
17. Bhattacharjee S. DLS and zeta potential, what they are and what they are not? J Control Release. 2016;235:337-351. doi:10.1016/j.jconrel.2016.06.017.
18. Modi S, Anderson BD. Determination of drug release kinetics from nanoparticles: overcoming pitfalls of the dynamic dialysis method. Mol Pharm. 2013;10(8):3076-3089. doi:10.1021/mp400154a.
19. Dixit P, Jain DK, Dumbwani J. Standardization of an ex vivo method for determination of intestinal permeability of drugs using everted rat intestine apparatus. J Pharmacol Toxicol Methods. 2012;65(1):13-17. doi:10.1016/j.vascn.2011.11.001.

20. Alam MA, Al-Jenoobi FI, Al-Mohizea AM. Everted gut sac model as a tool in pharmaceutical research: limitations and applications. J Pharm Pharmacol. 2012;64(3):326-336. doi:10.1111/j.2042-7158.2011.01391.x.
21. Volpe DA. Application of method suitability for drug permeability classification. AAPS J. 2010;12(4):670-678. doi:10.1208/s12248-010-9227-8.
22. Siepmann J, Peppas NA. Higuchi equation: derivation, applications, use and misuse. Int J Pharm. 2011;418(1):6-12. doi:10.1016/j.ijpharm.2011.03.051.
23. International Council for Harmonisation. Q1A(R2): Stability testing of new drug substances and products. Geneva: ICH; 2003.
24. International Council for Harmonisation. Q1E: Evaluation of stability data. Geneva: ICH; 2003.
25. Hathout EM, Eltokhy SS, Abdelkader DH, El Maghraby GM. Capryol-ethyl oleate self-microemulsifying system for improved intestinal absorption and hypoglycemic activity of empagliflozin. Pharm Dev Technol. 2026;31(5):778–793. doi:10.1080/10837450.2026.2674731.
26. Alam MA, Al-Jenoobi FI, Al-Mohizea AM. Everted gut sac model as a tool in pharmaceutical research: limitations and applications. J Pharm Pharmacol. 2012;64(3):326–336. doi:10.1111/j.2042-7158.2011.01391. x.
27. McClements DJ. Nanoemulsions versus microemulsions: terminology, differences, and similarities. Soft Matter. 2012; 8:1719–1729. doi:10.1039/C2SM06903B.
28. Alam S, Aeri V, Khan MI. A validated HPLC method for the quantification of oleanolic acid in the roots of Achyranthes aspera linn. and marketed formulation. International Journal of Pharmacy and Pharmaceutical Sciences. 2010; 2(1): 74-78.